### **Novel Surfactants**

Maximilian Eberhard Franke\* and Heinz Rehage

## Synthesis and characterisation of carboxy amidebonded pyridinium Gemini surfactants: influence of the nature of the spacer group and counterions on the aggregation behaviour

https://doi.org/10.1515/tsd-2021-2401 Received October 30, 2021; accepted December 8, 2021

**Abstract:** A series of novel dimeric pyridinium surfactants has been synthesised and the effects of a semi-flexible p-xylyl spacer and flexible, polyethylene glycol spacers have been studied. The nature of the spacer determines solubility and aggregation behaviour in two- and three-dimensional systems. Some of these insoluble compounds form twodimensional, rigid-condensed structures at the air-water interface, while others form liquid-analogue monolayers. Whereas the latter compounds become soluble after exchange of the counterions, the former remain insoluble. The aggregation behaviour of Langmuir layers was, inter alia, investigated by Brewster angle microscopy. The micellisation behaviour of diluted aqueous solutions of soluble surfactants was primarily investigated by conductometric measurements and thermodynamic parameters of aggregation have been deduced with respect to the spacer length.

**Keywords:** cationic Gemini surfactant; counterion effects; spacer effects; surfactant solubility.

## 1 Introduction

Cationic pyridinium surfactants consisting of amide functionalities linked to the charged head group represent a barely researched field in surfactant science. These types of surfactants are of special interest in terms of structure performance experiments, as their self-assembly is

\*Corresponding author: Maximilian Eberhard Franke, Lehrstuhl für Physikalische Chemie II, Technische Universität Dortmund, Dortmund, Germany, E-mail: maximilian.franke@tu-dortmund.de Heinz Rehage, Lehrstuhl für Physikalische Chemie II, Technische

E-mail: heinz.rehage@tu-dortmund.de

Universität Dortmund, Dortmund, Germany,

influenced by the ability to form hydrogen bond networks [1-3]. The rigid amide group, linked to the charged aromatic ring affects the orientation, which enhances the intermolecular interaction [4]. In polymer science, this effect explains the special properties of aramid polymers compared to aliphatic polyamides [5]. Monomeric chlorides of this type of surfactant are known to form hydrogels as result of these complex intermolecular forces [1]. Dimerisation of surfactants leads to a major enhancement of the surface-active properties [6–12]. Gemini surfactants of aramide bonded pyridinium surfactants combine the amplification of hydrophobic interaction resulting from dimerisation with the orienting effects of hydrogen bonding [2]. The spacer group, which connects the surfactant groups, significantly affects the aggregation behaviour [13-17]. Its nature in terms of length, polarity, rigidity and functionalisation shape the microstructures of the aggregates in bulk solutions [18-20] as well as in Langmuir layers [7]. Flexible polyoxyethylene-spacers, which do not significantly contribute to the hydrophobic interactions of cationic Gemini surfactants, influence aggregation depending on their length [21-23]. This allows to tune the micellisation properties and has been utilised for polymerisation in microemulsion in order to control the size of the polymer particles [23]. Packing parameters [24, 25] of micelles of Gemini surfactants depend on the spacer and the distance of the ionic groups as well as conformational isomerism [26] and affect the ionic head group interactions [20, 27], which contribute to the shape and stability of aggregates [28]. Ionisation parameters of micelles strongly depend on length and nature of the spacer [22, 29, 30]. Rigid p-xylyl spacers were found to decrease the solubility of cationic surfactants and lead to higher critical micelle concentrations (CMC) [20], whereas hydroxyl groups, which have a strong influence on the surrounding water molecules, promote the micellisation processes [22]. As we found in our own studies, Gemini surfactants, consisting of two amide groups attached to the cationic

heterocycle often led to insoluble compounds. Halides of this type are usually insoluble in water and most organic solvents, formates in contrast show a far better solubility [2]. This allows to investigate the aggregation behaviour in two-dimensional systems as well as in threedimensional systems. In both cases the nature of the spacer has been proven to be a crucial factor (Schemes 1 and 2).

## 2 Experimental procedure

### 2.1 Synthesis

All organic solvents were distilled before usage, high-purity water (Elga PURELAB flex) was always used. Glassware was treated by pyrolysis at 450 °C and rinsed with high-purity water. Formic acid was distilled under reduced pressure.

The precursor, *N*-(pyridin-3-yl)stearamide (P1) was synthesised as described by Brahmachari et al. [1]. Polyoxyethylene-dibromides were synthesised by treatment of the corresponding polyethylene glycols with phosphorus tribromide in dry dichloromethane and subsequent filtration and extraction of the dibromide with dichloromethane. The residue was at first washed with water, then with sodium carbonate solution and again with water for three times. Quarternisation of P1 with the polyoxyethylene-dibromides was performed by refluxing in acetonitrile over longer durations. The solvent was removed on a rotary evaporator to yield the stearamidopyridinium bromide Gemini surfactants Py<sub>2</sub>EO<sub>m</sub>Br. The reaction progress was monitored by TLC using a mixture of 94 wt% methanol, 3.5 wt% N,N-dimethylformamide and 0.5 wt% formic acid as eluent. After the reaction was finished, the solution was cooled to 10 °C and the raw product was washed with cold methanol. The product was recrystallised several times in methanol to yield the bromide forms as a white powder. The mother liquors of every step were collected and poured on a flash chromatography column with silica gel as adsorbent. The column was then washed with methanol until no spots of the eluate were detectable on a fluorescent marked TLC plate. Formic acid was used as eluent to rinse off the quarternary Gemini surfactant and the solvent was removed on a rotary evaporator afterwards. Ion exchange was performed by the usage of a strongly basic ion exchange resin to receive the pure formates, as described before [2]. The quarternisation of P1 with  $\alpha,\alpha'$ -dibromo-p-xylene was performed by heating to 70 °C in dry N,N-dimethylformamide for two

days. The residue was washed with methanol in an ultrasonic bath and filtrated several times. Ion exchange was performed in the same manner as for the polyoxyethylene surfactants.

### 2.2 Chemical characterisation

NMR measurements of the ionic compounds were performed in solvent mixtures containing deuterated formic acid, chloroform and N,N-dimethylformamide. This was necessary because of the strong aggregation properties of the compounds and resulting broaden of the signals, which was predominant in pure solvents. Coupling constants of <sup>1</sup>H NMR measurements could not be obtained due to the quality of the spectra. However, coupling was proved by 2D-NMR. The average spacer length of Py2EO3HCOO and Py2EO7HCOO, which were synthesised from polyethylene glycols, was proven by integration of the <sup>1</sup>H signals, Liquid chromatography–mass spectrometry measurements were performed on a Bruker compact QTOF including ESI ion-source, coupled to an Agilent 1260 HPLC-system.

Py<sub>2</sub>EO<sub>1</sub>HCOO-1,1'-((ethane-1,2-diylbis(oxy))bis(ethane-2,1-diyl)) bis(3-stearamidopyridine-1-ium) dimethanoate: <sup>1</sup>H NMR (CDCl<sub>3</sub>, DCOOD, DMF-d<sub>7</sub>, 25 °C, 400 MHz) δ [ppm]: 0.66-0.74 (6H) 1.06-1.17 (56H), 1.44-1.56 (4H), 2.25-2.39 (4H), 3.34-3.50 (4H), 3.73-3.87 (4H), 4.51-4.72 (4H), 7.71-7.48 (2H), 8.29-8.53 (4H), 9.35-9.50 (2H); <sup>13</sup>C NMR (CDCl<sub>3</sub>, DCOOD, DMF-d<sub>7</sub>, 25 °C, 100.64 MHz) δ [ppm]: 13.64, 22.21, 24.63, 29.23, 31.44, 36.42, 61.77, 68.67, 70.03, 127.62, 134.23, 134.50, 138.67, 139.45, 173.86.

Py<sub>2</sub>EO<sub>2</sub>HCOO-1,1'-(((oxybis(ethane-2,1-diyl))bis(oxy))bis(ethane-2,1-diyl))bis(3-stearamidopyridin-1-ium) dimethanoate: <sup>1</sup>H NMR (CDCl<sub>3</sub>, DCOOD, DMF-d<sub>7</sub>, 25 °C, 400 MHz) δ [ppm]: 0.72-0.78 (6H), 1.12-1.26 (56H), 1.52-1.61 (4H), 2.34-2.41 (4H), 3.41-3.43 (8H), 3.82-3.89 (4H), 4.60-4.68 (4H), 7.79-7.85 (2H), 8.39-8.45 (4H), 9.41-9.48 (2H); <sup>13</sup>C NMR (CDCl<sub>3</sub>, DCOOD, DMF-d<sub>7</sub>, 25 °C, 100.64 MHz) δ [ppm]: 13.78, 22.36, 24.79, 29.39, 31.60, 36.63, 61.87, 68.62, 69.77, 70.00, 127.75, 134.58, 134.69, 139.05, 139.42, 174.43; LC/MS: Base Peak: 440.6, Molecular Ion Peak: 880.0.

Py<sub>2</sub>EO<sub>3</sub>HCOO-1,1'-[poly(oxyethylene)]bis(3-stearamidopyridin-1-ium) dimethanoate ( $n \approx 3$ ): <sup>1</sup>H NMR (CDCl<sub>3</sub>, DCOOD, DMF-d<sub>7</sub>, 25 °C, 400 MHz) δ [ppm]: 0.69-0.77 (6H), 1.09-1.25 (56H),1.48-1.57 (4H), 2.29-2.38 (4H), 3.35-3.55 (12H), 3.81-3.91 (4H), 4.63-4.75 (4H), 7.82-7.88 (2H), 8.36–8.44 (2H), 8.46–8.54 (2H), 9.40–9.55 (2H); <sup>13</sup>C NMR (CDCl<sub>3</sub>, DCOOD, DMF-d<sub>7</sub>, 25 °C, 100.64 MHz) δ [ppm]: 12.97, 21.57, 24.03, 28.08-28.59, 30.82, 35.73, 61.02, 68.11, 69.20, 69.40, 126.99, 133.30-138.34, 138.94, 172.68.

Py<sub>2</sub>EO<sub>7</sub>HCOO-1,1'-[poly(oxyethylene)]bis(3-stearamidopyridin-1-ium) dimethanoate ( $n \approx 7$ ): <sup>1</sup>H NMR (CDCl<sub>3</sub>, 25 °C, 400 MHz)  $\delta$  [ppm]:

Scheme 1: Scheme of the structure of the surfactants. The counterions (X<sup>-</sup>) are bromide (Br<sup>-</sup>) or formate (HCOO<sup>-</sup>), the spacer group consists of a) a semi-flexible aromatic group referred to as Py2ArX or b) a flexible polyoxyethylene group with varying length (m = 1, 2,  $\approx$ 3,  $\approx$ 7) referred to as Py<sub>2</sub>EO<sub>m</sub>X.

Scheme 2: Synthesis process of the surfactants, including ion exchange and designation of the compounds.

0.82-0.87 (6H), 1.20-1.36 (56H), 1.63-1.72 (4H), 2.82-2.59 (4H), 3.40-3.77 (28H), 3.90-4.04 (4H), 4.64-4.77 (4H), 7.68-7.79 (2H), 8.31-8.60 (2H), 8.73-8.85 (2H), 9.09-9.40 (2H), 9.90-10.60 (2H); <sup>13</sup>C NMR (CDCl<sub>3</sub>, 25 °C, 127.71 MHz) δ [ppm]: 14.08, 22.65, 25.13, 29.20-29.67, 31.89, 36.92, 61.55, 69.08, 69.22, 69.35, 70.30, 70.48, 70.61, 127.29, 134.26, 134.10, 139.69, 139.01, 169.02, 175.11.

Pv2ArHCOO-1,1'-(1,4-phenylenebis(methylene))bis(3stearamidopyridin-1-ium) dimethanoate: <sup>1</sup>H NMR (CDCl<sub>3</sub>, DCOOD, DMF-d<sub>7</sub>, 25 °C, 500 MHz) δ [ppm]: 0.65–0.71 (6H), 1.05–1.19 (56H), 1.44-1.53 (4H), 2.30-2.37 (4H), 5.63-5.70 (4H), 7.37-7.41 (4H), 7.82-7.87 (2H), 8.29–8.35 (2H), 8.46–8.52 (2H), 9.43–9.47 (2H); <sup>13</sup>C NMR (CDCl<sub>3</sub>, DCOOD, DMF-d<sub>7</sub>, 25 °C, 100.64 MHz) δ [ppm]: 13.39, 22.05, 24.58, 28.52-29.09, 31.35, 36.69, 64.30, 128.42, 129.87, 134.39, 135.00, 138.87, 139.16, 175.16.

### 2.3 Physicochemical characterisation

Brewster angle microscopy (wavelength of the incident LASER beam 690 nm) and interfacial characterisation were performed on an Accurion Nanofilm Ultra BAM equipped with a Langmuir Blodgett trough, including a Wilhelmy plate and Kelvin probe (Kelvin probe KP1). Stock solutions of the samples were prepared by dissolving the amides in a 1/9 methanol/chloroform (v/v) mixture and spread via gastight glass syringe. Before starting the measurements, 20 min passed to allow the solvent to evaporate. All measurements were performed at 22 °C. Tensiometric measurements were performed on a DCAT 11 tensiometer (Dataphysics) equipped with a platinum-iridium Du Noüy ring at 22 °C. The ring was cleaned before each measurement by annealing on a Bunsen burner. Diluted solutions were stored over two days in the covered sample vessel and carefully placed into the tensiometer without concussions. The measurements were performed until no significant change of the surface tension over time was observed and the average plateau value was used. All measurements were performed twice to ensure reproducibility. Conductivity measurements were performed in a sealed vessel using a WTW Cond 7310 probe. High-purity water with a conductance of 18.2 M $\Omega$  cm was always used. Measurements of solutions of less than 1 mM surfactant were flushed with argon before sealing. The probe was cleaned in hot water by ultrasonic treatment. All samples were stirred during the measurement. Reproducibility was verified on a random basis. Dynamic light scattering experiments were performed on a Malvern

Zetasizer ZS nano instrument. Samples of micellar solutions were filtered through 0.2  $\mu$ m filters (VWR) to avoid interference with dust particles. These supplementary measurements were performed to confirm the micellisation data.

## 3 Results and discussion

## 3.1 Langmuir layers

The bromides of all compounds were found to be able to form stable Langmuir layers. Brewster angle micrographs of the film structures are shown in Figure 1. The textures of Langmuir films in the low compression range (at film pressures  $\pi$  of the film well below 1 mN/m) were found to be dependent on the nature of the spacer. Two-phase regions were observed: In case of Py<sub>2</sub>EO<sub>m</sub>Br two-dimensional foam analogue aggregates were found for all surfactants (see Figure 1b), which was interpreted as a two-phase region which involved a liquid analogue phase. In contrast, the Py<sub>2</sub>ArBr surfactant formed two-dimensional fractal-type aggregates, which indicates the formation of solid-analogue structures (Figure 1a). Further insights into lateral interactions of the surfactants were gained by pressure-area and surface potential-area isotherms and hysteresis experiments (see Figure 2). Although the *p*-xylyl spacer is the shortest, the film pressure increases at higher areas per molecule, which can be explained by the resistance of rigid, two-dimensional networks against compression, which leads to an increase of the film pressure as loosely packed films. The areas of increase of the film pressures of polyoxyethylene-linked surfactants correspond to their spacer length. Noticeable hysteresis effects were observed for the  $Py_2ArBr$  surfactant even without preceding film collapse, while only minor hysteresis effects were observed for the  $Py_2EO_mBr$  surfactants (see Figure 2b). For  $Py_2ArBr$ , the surface potential increases noticeably with compression even before formation of a packed Langmuir film, while for  $Py_2EO_mBr$  a sudden increase was observed when a condensed film evolved. This increase might be the area, at which the two-phase foam analogue area is compressed into one homogenous layer. Consequently, the lateral interactions are considerably influenced by the nature of the spacer.

In order to find out more about the effects of the backbone structure without ionic contributions, we studied insoluble films of the precursor P1 of the surfactants. Although the structure is similar to that of long chain fatty acids or alcohols it was found that the formation of twodimensional crystalline aggregates is favoured and already occurs at very low film pressures of less than 5 mN/m (see Figures 1c and 2). The absence of ionic repulsion explains the stronger tendency to form two-dimensional crystalline structures. This can be explained by the nature of the amide functionality. In contrast to ester bonds, which are structural similar to amides, hydrogen donors and acceptors are present. As a result, the cohesive forces are much stronger in case of an amide. A simple example is the difference in the boiling temperature of ethyl acetate and N-ethylacetamide: Although the structure is similar and the molecular mass of the ester and the amide is nearly the

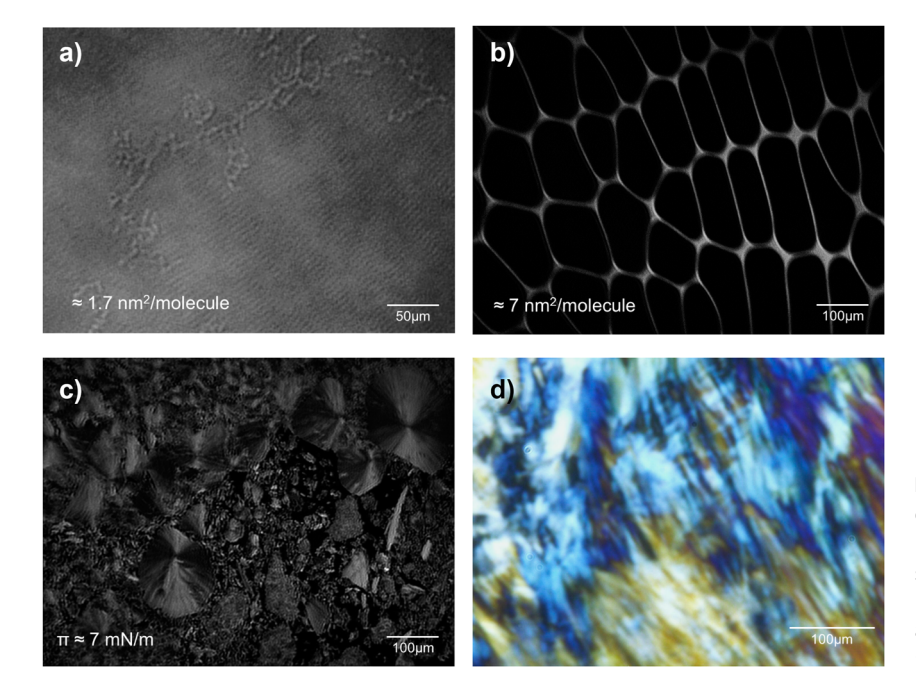
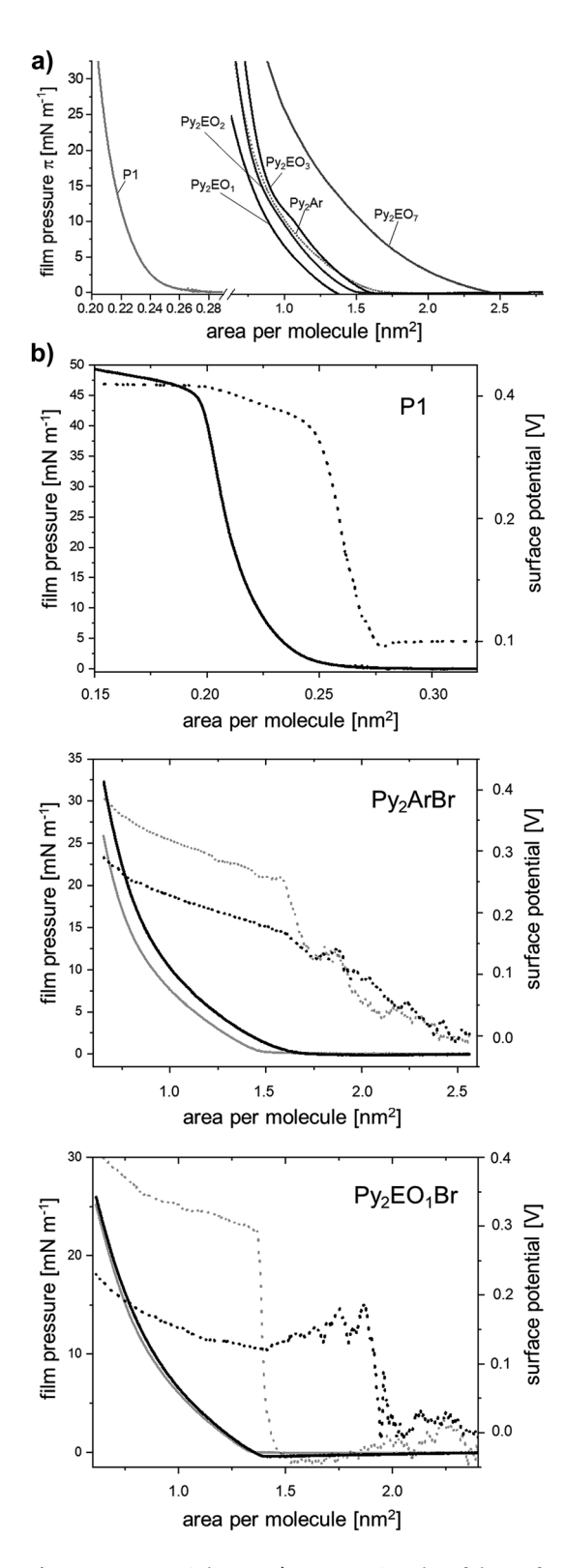


Figure 1: Brewster angle micrographs of twodimensional aggregates: a) Py<sub>2</sub>ArBr and b) Py<sub>2</sub>EO<sub>7</sub>Br, expended films before compression; c) P1 at moderate film compression. d) Photomicrograph of textures of aqueous 80 wt% Py<sub>2</sub>EO<sub>7</sub>HCOO obtained in crosspolarised light.



**Figure 2:** Langmuir layers: a) Comparative plot of the surface pressure versus area isotherms of the Gemini surfactants and the precursor on water, b) Surface pressure versus area (solid) and surface potential versus area (dashed) isotherms of the surfactant bromides ( $Py_2EO_1Br$  representing the polyoxyethylene-linked surfactants) and the precursor on water. The grey lines indicate the hysteresis measurement after 45 min of film regeneration time at maximal expansion. Temperature of measurements: 22 °C.

same, the boiling temperature of the amide is about 150 K higher. This effect can also be present in case of monolayers, if the structural geometry of the molecules enables hydrogen bonding, in addition to the lateral van der Waals forces.

## 3.2 Solubility and counterion

The counterion has a significant influence on the solubility of the surfactants. As the long-time stability of the Langmuir layers proves, bromides are insoluble compounds for both types of spacers. The exchange of the counterion into formates leads to a significant improvement of the solubility: The Py2ArHCOO surfactant becomes soluble in methanol but remains insoluble in water at room temperature. The Krafft point, which was not further investigated, was found to be over 80 °C. However, the Py<sub>2</sub>EO<sub>m</sub>HCOO surfactants become water-soluble, even at high concentrations. The formation of textures, typical for liquid crystals could be obtained under polarised light at high concentrations. Figure 1d shows a structure, which may be regarded as hexagonal liquid crystal phase. LC-phases were found for all Py2EOmHCOO surfactants. It is therefore conceivable that the formate counterion, which is a charged hydrogen bond acceptor, interacts with the hydrogen bond network of the amide bonds and leads to an amelioration of solvation.

# 3.3 Effect of the spacer on the aggregation in aqueous solution

Detailed investigation of the micellisation properties was conducted for the  $Py_2EO_mHCOO$  series by tensiometry and conductivity measurements. The results were confirmed by dynamic light scattering as a complementary method. Because of the high Krafft temperatures, the aggregation properties of  $Py_2ArHCOO$  in aqueous solution were not further investigated.

### 3.3.1 Tensiometry

The length of the polyoxyethylene spacer has a significant effect on the adsorption at the air—water interface (see Figure 3). Shorter spacers lead to a higher charge density, which enforces electrostatic repulsion [31]. It was found that the lowering of the surface tension of the surfactants with longer spacers is greater and that short-spacer surfactants reduce the surface tension of water even at very low concentrations. However, the adsorption process was ongoing for many hours, especially at lower concentrations. This

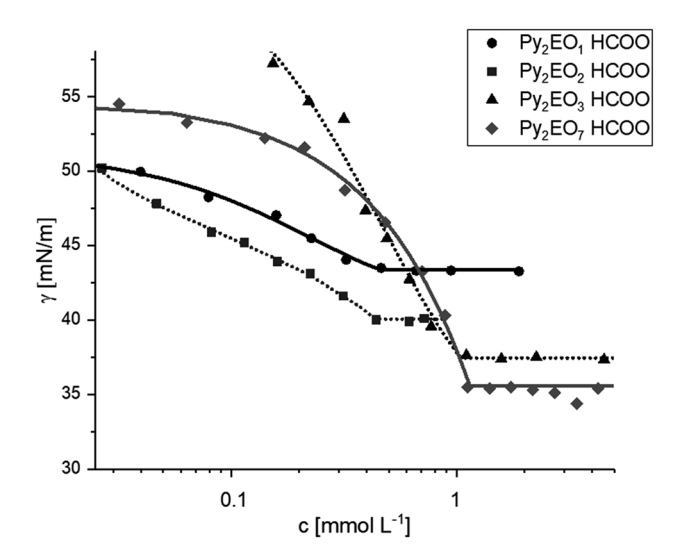


Figure 3: Surface tension  $\gamma$  against concentration of aqueous solutions of the  $Py_2EO_mHCOO$  at 22 °C.

behaviour has been often found for cationic surfactants [7] and impedes the conduction of tensiometric experiments. The basicity of the formate counterion is many orders of magnitude larger than those of commonly used counterions as halides, therefore the association-dissociation equilibrium complicates the analysis of the Gibbs adsorption layer [31]. We found that the linear range of the Gibbs isotherms in the semi-logarithmic plot is rather narrow. The spacer length determines the maximal lowering of the surface tension  $y_{CMC}$  and also the slope of the Gibbs isotherm in the y versus log (c) plot. Because of the uncertainty of dissociation in the Gibbs adsorption layers of the pyridinium amide formats, the surface excess could not be determined with sufficient reliability. However, if the slopes of the linear ranges of the Gibbs isotherms in the semi-logarithmic plot are compared, a clear trend can be found: the shorter Py<sub>2</sub>EO<sub>2</sub>HCOO has a maximal slope, which is in absolute values about 10% higher than that of Py<sub>2</sub>EO<sub>1</sub>HCOO, in case of Py<sub>2</sub>EO<sub>3</sub>HCOO it is about twice as high and for Py<sub>2</sub>EO<sub>7</sub>HCOO it is four times higher. The shorter spacers of Py<sub>2</sub>EO<sub>1</sub>HCOO and Py<sub>2</sub>EO<sub>2</sub>H-COO are consequently stronger hindered in the formation of a Gibbs adsorption layer by electrostatic repulsion, have a lower surface excess and a minor lowering of the surface tension at the CMC.

#### 3.3.2 Conductivity measurements

The specific conductivities with concentration at temperatures between 10 °C and 60 °C are shown in Figure 4. It is particularly noteworthy that at very low concentrations, we found nonlinear behaviour at higher temperatures. This indicates an interaction of the ionic groups that starts even

at very low concentrations. The interaction occurs at lower temperatures and is reduced by an increase of the temperature. This results in a stronger increase of the ion mobility and therefore a non-linear increase of the conductivity with temperature. This behaviour could be found for all  $Py_2EO_mHCOO$  surfactants and might be a result of ion pairing at lower temperatures [10]. The amide group of the surfactant ion serves as hydrogen donor and is located in the vicinity of the cationic heterocycle, while the carboxyl group of the counterion is a hydrogen acceptor, therefore a type of localised hydrolysis [32] could explain this behaviour. In order to describe the specific conductivity with concentration, we used a modified Carpena [33] fit function:

$$F(x) = \sigma_0 + (\sigma_1' \cdot x) + x_1 \cdot (\sigma_2' - \sigma_1') \cdot \ln\left(\frac{1}{2} + \frac{1}{2} \exp\left(\frac{x}{\Delta x_1}\right)\right)$$
$$+ (\sigma_2' \cdot x) + x_2 \cdot (\sigma_3' - \sigma_2') \cdot \ln\left(\frac{1 + \exp\left(\frac{x - CMC}{\Delta x_2}\right)}{1 + \exp\left(\frac{-CMC}{\Delta x_2}\right)}\right)$$
(1)

This function takes the nonlinear behaviour at very low concentrations into account and yielded very good agreement with the experimental points of measurement (coefficient of determination >0.99998). The second derivative of Eq. (1) was used to describe the aggregation behaviour of the surfactants. Figure 5 indicates the deviation from linear behaviour (dark colour) and contains information about the latitude of the transition ranges. The white areas indicate linear behaviour of the specific conductivity with

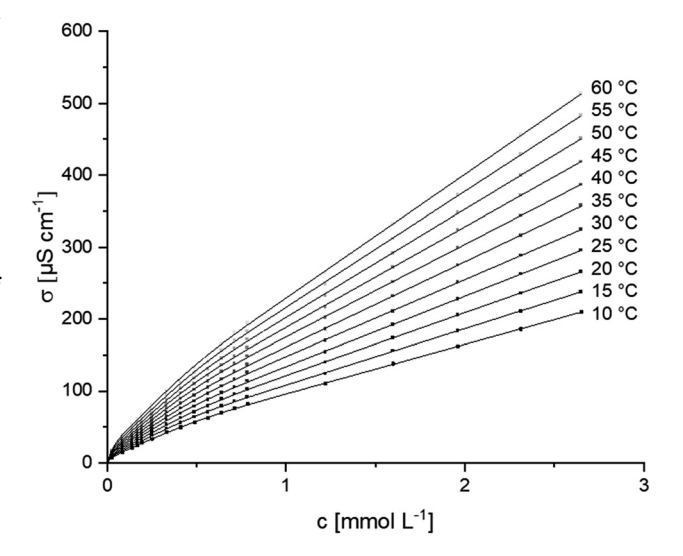


**Figure 4:** Specific conductivity  $\sigma$  against concentration and temperature of aqueous solutions of Py<sub>2</sub>EO<sub>1</sub>HCOO (illustrative for all polyoxyethylene-linked surfactants) and fit functions at given temperature (see text).

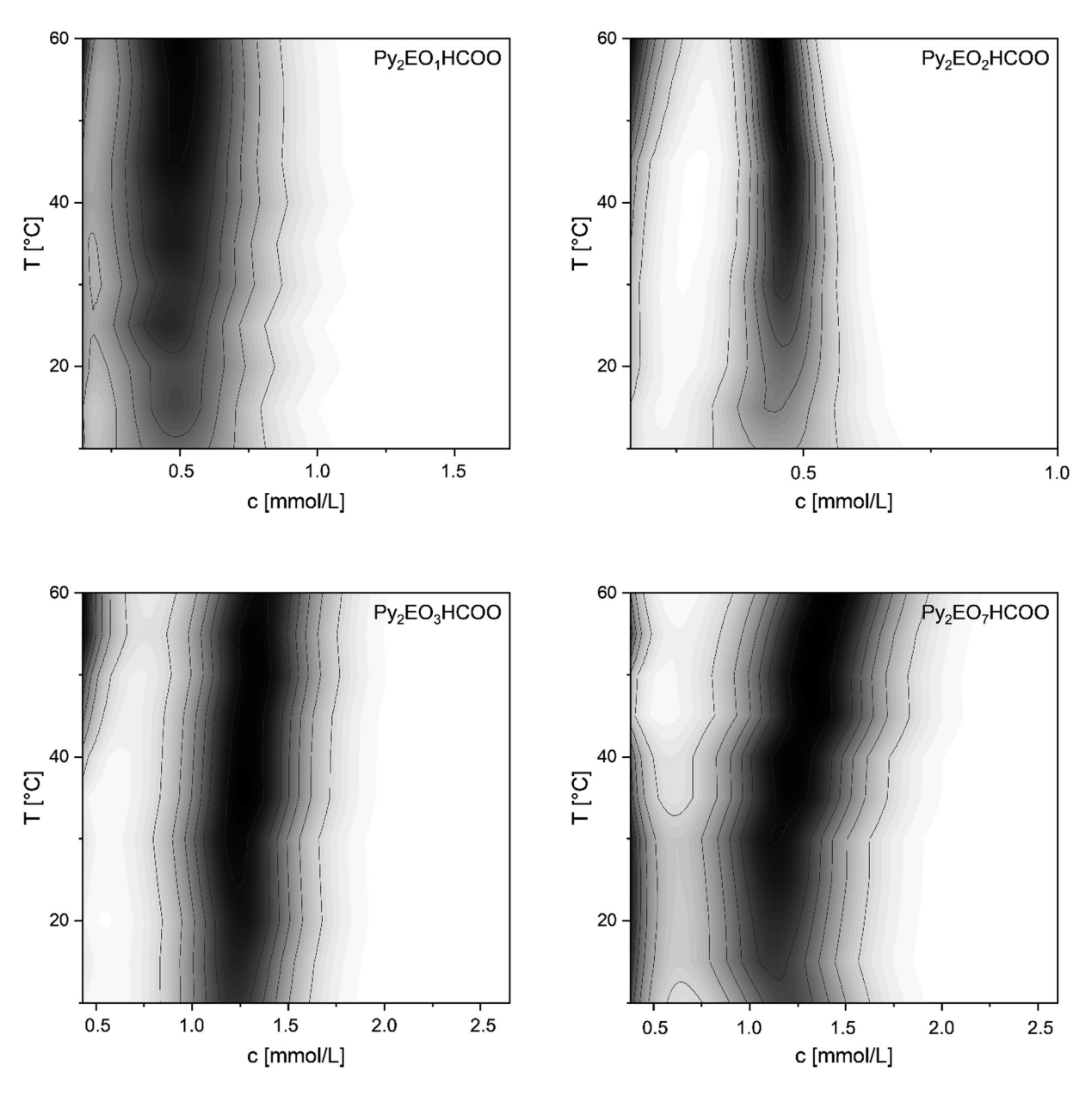


Figure 5: Phase diagrams of the Py<sub>2</sub>EO<sub>m</sub>HCOO of the low concentration regime, including the transition areas of micellisation, which were determined by Carpena fits. The grey levels indicate the normalised deviation from linear behaviour.

concentration and therefore regions where no phase transition takes place. Figure 6a) compares in addition to Figure 5 the CMC of the surfactants in one plot.

### 3.3.3 Thermodynamics of micellisation

The data obtained from the Carpena fit functions were utilised to obtain thermodynamic parameters for micellisation. The counterion dissociation of micelles was estimated by

$$\alpha = \frac{\sigma_2' + \sigma_3'}{2\sigma_2'} \,. \tag{2}$$

The Gibbs energy of micellisation  $\Delta G_m$  could be determined by Eq. (3) [34]

$$\Delta G_m = 2RT (1.5 - \alpha) \ln (X_{CMC}), \qquad (3)$$

where  $X_{CMC}$  denotes the mole fraction of Gemini surfactant at the CMC, R is the gas constant and T the absolute temperature. The enthalpy of micelle formation  $\Delta H_m$  was derived by the van't Hoff equation (Eq. (4)).

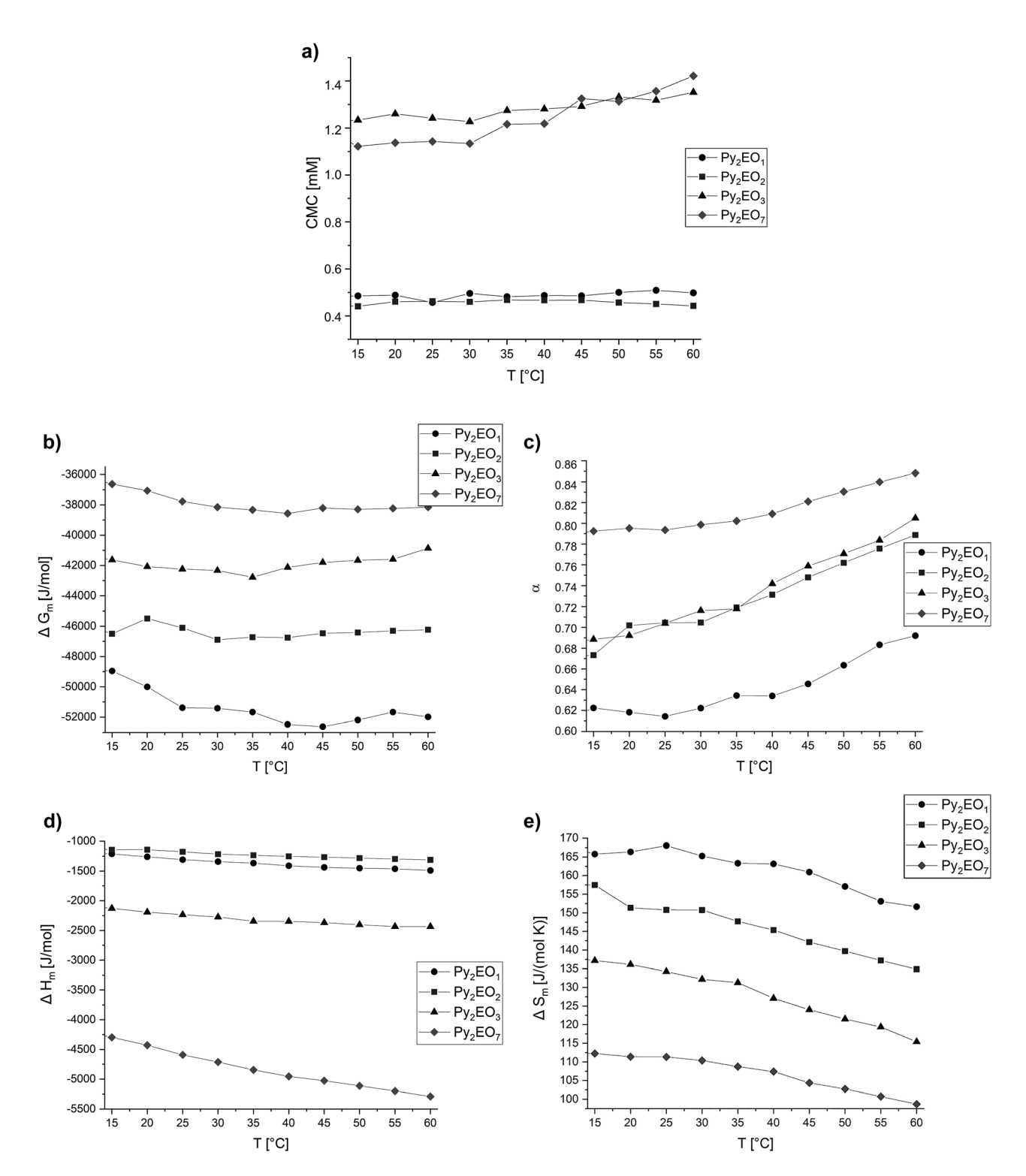


Figure 6: Micellisation data obtained from the conductivity measurements at a temperature range of 15 °C-60 °C.

$$\Delta H_m^0 = -2RT^2 (1.5 - \alpha) \left( \frac{\delta \ln (X_{CMC})}{\delta T} \right)_p \tag{4}$$

The term  $\frac{\delta \ln(X_{CMC})}{\delta T}$  was received by usage of the fit functions of the CMC curve. The entropy of micellisation  $\Delta S_m^0$  was calculated by Eq. (5):

$$\Delta S_m^0 = \frac{\Delta H_m^0 - \Delta G_m^0}{T} \ . \tag{5}$$

The CMC of the Py2EOmHCOO varies by a factor of three, depending on the spacer length and tends to increase with the length of the polyoxyethylene spacers. The CMC of the two short-chain surfactants (see Figure 6a) has similar values over the observed temperature range. However, the transition width in relation to the CMC is greater for the short-chain Py<sub>2</sub>EO<sub>1</sub>HCOO (see Figure 5), which might result from higher charge density. The CMC values of the surfactants with longer spacers (m  $\approx$  3 and m  $\approx$  7) are considerably higher. The temperature dependence of micellisation is also significantly affected by the spacer length: The CMC of Py<sub>2</sub>EO<sub>1</sub>HCOO and Py<sub>2</sub>EO<sub>2</sub>HCOO remains almost constant with temperature, while Py<sub>2</sub>EO<sub>3</sub>HCOO and Py<sub>2</sub>EO<sub>7</sub>HCOO increase moderately. The entropy of micellisation  $\Delta S_m^0$  decreases with an increasing number of oxyethylene groups (see Figure 6e). The counterion dissociation of micelles a increases with larger spacer length and temperature for all Py<sub>2</sub>EO<sub>m</sub>HCOO (see Figure 6c). Higher charge density of the short-chain surfactants can explain the order of the  $\alpha$  values with spacer length: It leads to stronger electrostatic forces on the surface of the micelle and results in stronger bound counterions. In accordance with this, the  $\Delta H_m$  values of short-spacer surfactants are considerably lower in absolute values (less exothermic) resulting from higher electrostatic repulsion between surfactant head groups. The entropy of micellisation  $\Delta S_m^0$  is higher for surfactants with shorter spacers. This might be an indication of the occurrence of intramolecular alkyl chain condensation, which is more likely, if flexible spacers are long enough to allow contact of the alkyl chains in solution [10]. As result of these effects, the  $\Delta G_m$  values become more negative with shorter spacers. The CMC values of the Py<sub>2</sub>EO<sub>1</sub>HCOO and the Py<sub>2</sub>EO<sub>2</sub>HCOO are more than twice as high than those of comparable dimeric pyridinium amide formates with short hydrophilic spacers and only six linking atoms between the cationic pyridinium heterocycle [2]. The micellar counterion dissociation of Py<sub>2</sub>EO<sub>1</sub>HCOO with only eight linking atoms, as well as all other surfactants with longer polyoxyethylene spacers, is considerably higher. The micellisation is for the reasons mentioned above less exotherm and the free energy of micellisation is significantly lower on absolute values, as well

as the entropy of micellisation. It can therefore be concluded that the electrostatic effects have a considerable influence on the aggregation, especially for short-spacer surfactants.

## 4 Conclusions

The effects of the nature of the spacer, as well as counterion effects have been studied. It was found that bromides possess poor solubilities, even with long polyoxyethylene spacers and can form stable Langmuir layers. The behaviour of two-dimensional aggregates is strongly dependent on the nature of the spacer. We found the formation of rigid, branched aggregates at low film pressures of the Gemini surfactant with semi-flexible spacer, while the surfactants with polyoxyethylene spacers form liquid analogue aggregates. The nonionic precursor, which forms stable Langmuir layers, shows the tendency to form twodimensional solid condensed films at low surface pressures. The formation of two-dimensional solid structures indicates strong lateral cohesive forces which can be explained by the presence of hydrogen donors and acceptors. The solubility behaviour changes dramatically with exchange of the counterion into the formate, which is probably the result of an alteration of the hydrogen bonding network by the hydrogen accepting counterion. The p-xylyl-linked surfactant becomes soluble in methanol but remains insoluble in water at room temperature. In contrast, surfactants with polyoxyethylene spacers are well soluble in water and exhibit lyotropic behaviour at high concentrations. Micellisation properties of the polyoxyethylene-linked surfactants as well as the adsorption at the water surface are significantly affected by the length of the polyoxyethylene spacer. The dependence of the micellisation parameters on the spacer length agrees with the results of comparable cationic quaternary ammonium Gemini surfactants [21, 22]. Most effects can be explained by electrostatic considerations: Shorter spacers lead to a higher charge density within a surfactant divalent cation. This leads to stronger binding of counterions and reduces the enthalpy of aggregation. The entropic contribution of micellisation is higher for shorter spacers, as premicellar aggregation and intramolecular alkyl chain condensation are impeded by stronger electrostatic repulsion.

Author contribution: All the authors have accepted responsibility for the entire content of this submitted manuscript and approved submission.

Research funding: None declared.

Conflict of interest statement: The authors declare no conflicts of interest regarding this article.

## References

- 1. Brahmachari S., Debnath S., Dutta S., Das P. K. Pyridinium based amphiphilic hydrogelators as potential antibacterial agents. Beilstein J. Org. Chem. 2010, 6, 859-868; https://doi.org/10. 3762/bjoc.6.101.
- 2. Franke M. E., Rehage H. Effects of chirality on the aggregation properties of amide-bonded pyridinium gemini surfactants. Langmuir 2019, 35, 8968-8976; https://doi.org/10.1021/acs. langmuir.9b00592.
- 3. Zhu Z., Lu X., Lin L., Xu H., Gao H. Synthesis and properties of cationic gemini surfactants with amide groups. Tenside Surfactants Deterg. 2020, 57, 332-339; https://doi.org/10.3139/ 113.110690.
- 4. Ballauff M. Flüssig-kristalline polymere. Chem. Unserer Zeit 1988, 2, 63; https://doi.org/10.1002/ciuz.19880220204.
- 5. Machalaba N. N., Perepelkin K. E. Heterocyclic aramide fibersproduction principles, properties, and application. J. Ind. Text. 2002, 31, 189-204; https://doi.org/10.1101/152808302026484.
- 6. Menger F. M., Littau C. A. Gemini-surfactants: synthesis and properties. J. Am. Chem. Soc. 1991, 113, 1451-1452; https://doi. org/10.1021/ja00004a077.
- 7. Menger F. M., Littau C. A. Gemini surfactants: a new class of selfassembling molecules. J. Am. Chem. Soc. 1993, 115, 10083-10090; https://doi.org/10.1021/ja00075a025.
- 8. Sidim T., Akbaş H. Thermodynamic and interfacial properties of cationic gemini surfactant in the presence of alcohols. Tenside Surfactants Deterg 2018, 55, 287; https://doi.org/10.3139/113. 110565.
- 9. Liu J., Hu M., Xie Y., Xu H. Study on a class of cationic gemini surfactants. Tenside Surfactants Deterg. 2019, 56, 319-326; https://doi.org/10.3139/113.110628.
- 10. Zana R., Xia J. Gemini Surfactants: Synthesis, Interfacial and Solution-Phase Behavior, and Applications, Surfactant Science, Vol. 117; Marcel Dekker, INC.: New York, Basel, 2003.
- 11. Sharma V. D., Ilies M. A. Heterocyclic cationic gemini surfactants: a comparative overview of their synthesis, self-assembling, physicochemical, and biological properties. Med. Res. Rev. 2014, 34, 1-44; https://doi.org/10.1002/med.21272.
- 12. Kumar N., Tyagi R. Industrial applications of dimeric surfactants. J. Dispers. Sci. Technol. 2014, 35, 205-214; https://doi.org/10. 1080/01932691.2013.780243.
- 13. Zana R., Benrraou M., Rueff R. Alkanediyl-alpha, omegabis(dimethylalkylammonium bromide) surfactants. 1. Effect of the spacer chain-length on the critical micelle concentration and micelleionization degree. Langmuir 1991, 7, 1072-1075; https:// doi.org/10.1021/la00054a008.
- 14. Zana R. Dimeric (gemini) surfactants: effect of the spacer group on the association behavior in aqueous solution. J. Colloid Interface Sci. 2002, 248, 203-220; https://doi.org/10.1006/jcis.2001.8104.
- 15. Mobin M., Aslam R. Ester-based pyridinium gemini surfactants as novel inhibitors for mild steel corrosion in 1 M HCl solution. Tenside Surfactants Deterg 2017, 54, 486-499; https://doi.org/ 10.3139/113.110527.
- 16. Song L. D., Rosen M. J. Surface properties, micellization, and premicellar aggregation of gemini surfactants with rigid and flexible spacers. Langmuir 1996, 12, 1149-1153; https://doi.org/ 10.1021/la950508t.

- 17. Rosen M. J., Mathias J. H., Davenport L. Aberrant aggregation behavior in cationic gemini surfactants investigated by surface tension, interfacial tension, and fluorescence methods. Langmuir 1999, 15, 7340-7346; https://doi.org/10.1021/ la9904096.
- 18. Maiti P. K., Chowdhury D. Micellar aggregates of gemini surfactants: Monte Carlo simulation of a microscopic model. Europhys. Lett. 1998, 41, 183-188; https://doi.org/10.1209/epl/ i1998-00128-3.
- 19. Zana R., Talmon Y. Dependence of aggregate morphology on structure of dimeric surfactants. Nature 1993, 362, 228-230; https://doi.org/10.1038/362228a0.
- 20. Wang X., Wang J., Wang Y., Yan H., Li P., Thomas R. K. Effect of the nature of the spacer on the aggregation properties of gemini surfactants in an aqueous solution. Langmuir 2004, 20, 53-56; https://doi.org/10.1021/la0351008.
- 21. Dreja M., Pyckhout-Hintzen W., Mays H., Tieke B. Cationic gemini surfactants with oligo(oxyethylene) spacer groups and their use in the polymerization of styrene in ternary microemulsion. Langmuir 1999, 15, 391-399; https://doi.org/10.1021/ la981354v.
- 22. Wettig S. D., Li X., Verrall R. E. Thermodynamic and aggregation properties of gemini surfactants with ethoxylated spacers in aqueous solution. Langmuir 2003, 19, 3666-3670; https://doi. org/10.1021/la0340100.
- 23. Dreja M., Tieke B. Polymerization of styrene in ternary microemulsion using cationic gemini surfactants. Langmuir 1998, 14, 800-807; https://doi.org/10.1021/la9710738.
- 24. Israelachvili J. N., Mitchell D. J., Ninham B. W. Theory of selfassembly of hydrocarbon amphiphiles into micelles and bilayers. J. Chem. Soc., Faraday Trans. 1976, 272, 1525–1568; https://doi. org/10.1039/f29767201525.
- 25. Israelachvili J. N. Intermolecular and Surface Forces; Elsevier: Amsterdam, Vol. 3, 2011.
- 26. Kamal M. S., Shakil Hussain S. M., Fogang L. T., Sultan A. S. Impact of spacer and hydrophobic tail on interfacial and rheological properties of cationic amido-amine gemini surfactants for EOR application. Tenside Surfactants Deterg. 2018, 55, 491; https://doi.org/10.3139/113.110591.
- 27. Tsubone K., Ghosh S. Micelle ionization degree of anionic gemini surfactant having N,N-dialkylamide and carboxylate groups. J. Surfactants Deterg. 2003, 6, 225-229; https://doi.org/10. 1007/s11743-003-0265-2.
- 28. Sorrenti A., Illa O., Ortuno R. M. Amphiphiles in aqueous solution: well beyond a soap bubble. Chem. Soc. Rev. 2013, 42, 8200-8219; https://doi.org/10.1039/c3cs60151j.
- 29. Borse M., Sharma V., Aswal V. K., Goyal P. S., Devi S. Effect of head group polarity and spacer chain length on the aggregation properties of gemini surfactants in an aquatic environment. J. Colloid Interface Sci. 2005, 284, 282-288; https://doi.org/10. 1016/j.jcis.2004.10.008.
- 30. Alami E., Beinert G., Marie P., Zana R. Alkanediyl-α, ω-bis(dimethylalkylammonium bromide) surfactants. 3. Behavior at the air-water interface. Langmuir 1993, 9, 1465-1467; https:// doi.org/10.1021/la00030a006.
- 31. Phan C. M., Le T. N., Nguyen C. V., Yusa S.-i. Modeling adsorption of cationic surfactants at air/water interface without using the Gibbs equation. Langmuir 2013, 29, 4743-4749; https://doi.org/ 10.1021/la3046302.

- 32. Robinson R. A., Harned H. S. Some aspects of the thermodynamics of strong electrolytes from electromotive force and vapor-pressure measurements. Chem. Rev. 1941, 28, 419-476; https://doi.org/10.1021/cr60091a001.
- 33. Carpena P., Aguiar J., Bernaola-Galván P., Ruiz C. Problems associated with the treatment of conductivity-concentration data in surfactant solutions: simulations and experiments. Langmuir 2002, 18, 6054-6058; https://doi.org/10.1021/la025770y.
- 34. Zana R. Critical micellization concentration of surfactants in aqueous solution and free energy of micellization. Langmuir 1996, 12, 1208-1211; https://doi.org/10.1021/la950691q.

## **Bionotes**

#### Maximilian Eberhard Franke

Dr. Maximilian Eberhard Franke studied chemistry at the Heinrich Heine University Düsseldorf and at the Technical University of Dortmund. He specialised in physical chemistry of colloids and

interfaces as well as in surfactant synthesis. In 2019, he obtained his doctorate with a thesis on novel types of pyridinium Gemini surfactants. He is currently working in research and development on surfactants for commercial applications.

### Heinz Rehage

Prof. Dr. Heinz Rehage studied chemistry at the universities of Clausthal-Zellerfeld, Göttingen and Bayreuth. After completing his studies, he spent one year at the "Collège de France" in Paris. In 1991, he was appointed to the "Hans-Goldschmidt-Stiftungsprofessur" at the University of Duisburg-Essen. In 2004, he received a new position as C4-full professor at the Technical University of Dortmund, where he worked in the field of "Physical Chemistry", "Colloid Chemistry" and "Surface and Surfactant Science" until his retirement in 2018. Prof. Rehage was member of the boards of numerous committees, including the German "Colloid Society", the IUPAC commission "Oil, Fats and Derivatives" and the GDCH-working group "Chemistry of Washing". From 2009 to 2012 he was Dean of the Faculty "Chemistry and Chemical Biology" at TU Dortmund University.